Composites Part B 149 (2018) 165–177

Contents lists available at ScienceDirect

Composites Part B

journal homepage: www.elsevier.com/locate/compositesb

Quasi-static compressive response of compression molded glass microballoon/HDPE syntactic foam

M.L. Jayavardhan, Mrityunjay Doddamani*

Lightweight Materials Laboratory, Department of Mechanical Engineering, National Institute of Technology Karnataka, Surathkal, India

ARTICLE INFO

Keywords:
Syntactic foam
Glass microballoon
HDPE
Quasi-static compression
Porfiri-Gupta model

ABSTRACT

Quasi-static compressive behavior of different density glass microballoon (GMB) reinforced high density polyethylene (HDPE) syntactic foams are investigated in the present work. Reducing the weight of thermoplastic components has been always a high priority in transportation, aerospace, consumer products and underwater vehicle structures. Despite continued interest in developing lightweight thermoplastic syntactic foams, they have not been studied extensively for quasi-static response with focus on wall thickness and volume fraction variations. Compression molded GMB/HDPE sheets are subjected to 0.001, 0.01 and 0.1 s^{-1} strain rates. Compressive modulus of foams is higher compared to neat HDPE. Increasing strain rates and decreasing filler content increases yield strength for all the foams investigated compared to neat HDPE. Yield strain and energy absorption of GMB/HDPE foams increases with an increasing strain rate and wall thickness. Specific modulus and strength of GMB/HDPE foams are superior and are comparable to neat HDPE. GMB/HDPE foam achieved high stiffness to weight ratio making them suitable for wide variety of applications. Theoretical model based on differential scheme predicts a good estimate of elastic modulus for all the type of GMB/HDPE foams. Finally, property map is exhibited to present comparative studies with existing literature.

1. Introduction

Contribution of inorganic solid fillers towards growth of the thermoplastic industry is phenomenal. Initially fillers are introduced to replace expensive resin with primary objective of cost reduction [1]. Researchers over time explored filler usage in providing tailored unique properties to these plastics alongside functional benefits. Fillers modify thermal, mechanical, magnetic, electrical and surface properties [2]. They can also act as fire retardants [3] and processing aids and stabilizers [4]. More than one property is modified by fillers in most of the cases. Solid fillers are having higher density than the neat resin making plastic components to gain weight substantially. Advent of glass microballoons (GMBs) in 1960s changed the scenario the way lightweight materials are designed and developed [5]. Making lightweight thermoplastics parts has been a high-priority in industries like handheld electronics, sports, aerospace, transportation and leisure. GMBs find numerous applications in variety of applications in automotive sector including sheet, thermoplastics and bulk molding composites, structural foams, plastisols and auto body fillers. GMBs are promising candidate materials in developing lightweight thermoplastic composites with price advantage without compromising mechanical properties [6]. Several benefits imparted by GMBs include higher modulus, dimensional stability, heat distortion resistance, reduced thermal conductivity and dielectric constant [1]. Such benefits of GMBs when infused in thermoplastic matrix for weight sensitive applications can be commercialised easily by using existing industrial scale compression molding machines.

Weight sensitive applications strive for better strength, toughness and damage tolerant low density material systems. Such lightweight composites are developed by dispersing hollow particles in matrix resin, called as syntactic foams [5]. Under compressive loading such foam composites exhibit considerable densification owing to in-situ porous microstructure providing higher failure strain [7–9]. Matrix reinforcements in particulate form permit lower processing cost, improvement in mechanical properties, high dimensional stability and wear resistance [10]. The ability of tailoring the mechanical properties of syntactic foams for a specific application is dependent on choice of appropriate matrix and hollow microballoons. Metals, polymers or ceramics as matrix and cenospheres, glass, phenolic, carbon and polymer microspheres as fillers are widely used to tune the syntactic foam properties. Thermoplastic polymers are most commonly used matrix by usage in cost sensitive markets [11]. Glass microsphere is a more versatile inorganic filler compared to other hollow filler, because it develops a product incorporated properties such as low density, improved

* Corresponding author.
E-mail address: mrdoddamani@nitk.edu.in (M. Doddamani).

https://doi.org/10.1016/j.compositesb.2018.04.039
Received 17 January 2018; Received in revised form 9 March 2018; Accepted 19 April 2018
Available online 24 April 2018
1359-8368/

Table 1
Physical properties of HDPE used in the study.[a]

Properties	Value
Melt flow index	20g/10 min
Density @ 23 °C	0.950 g/cm^3
Tensile yield strength	22 MPa
Elongation at yield	12%
Flexural Modulus	750 MPa
Hardness	55 shore D
Vicat Softening Point (10 N)	124 °C

[a] As supplied by Indian Oil Corporation Ltd., Mumbai, India.

dimensional stability, increased impact strength, smoother surface finish, greater thermal insulation, easier machinability, faster cycle times and cost savings [12–14].

Thermoset matrices with GMBs are widely investigated in recent past. GMBs prevent crack propagation in the matrix by absorbing more energy under compressive loading providing mechanical properties enhancement [15]. Primarily, debonding, crack bowing and crack deflection are the failure mechanisms observed in syntactic foams [16]. Swetha and Ravikumar [15] investigated the hollow glass microsphere reinforced epoxy syntactic foam and reported compression strength and modulus decreases with the increase in wall thickness of microsphere. Numerous works are published on mechanical, thermal properties of glass microsphere/thermoset foams [15,17–19]. Semi-structural and engineering applications prefer thermoplastics being recyclable, reusable and mouldable in to different shapes. Their current and future applications are driven by processing flexibilities using variety of industrial scale manufacturing techniques. Among available thermoplastic materials, HDPE is the most consumed in fabrication of products such as beverage bottles, storage bins, automotive molded parts and casting for consumer electronic items [20]. Hollow microballoons if imbibed in such matrix, may reduce the consumption of such expensive matrix in addition of imparting useful specific properties. Recently authors presented unique approach of developing HDPE syntactic foams using naturally available fly ash cenosphere through injection molding route [21–23] and GMBs using compression molding technique [6]. Syntactic foams exhibit superior response when loaded under compression mode owing to large densification values. Nevertheless, to the best of author's knowledge effect of wall thickness, volume fraction and strain rate variations are not investigated for industrial scale compression molded GMB/HDPE thermoplastic foams. Recent studies [15,16,21] reveals the effect of strain rate on mechanical properties of the syntactic foams. Syntactic foams are loaded at low strain rate in quasi static mode to characterize the damage evolution, failure features and energy absorbing capacities [15,21,24–27]. Thereby, present work deals with investigating quasi-static compressive response of GMB/HDPE syntactic foams synthesized using compression molding. Constituent materials are used in as received conditions. Interface mechanism between the constituents plays a crucial role in tensile and flexural properties compared to compressive behavior [21,28–30] as during deformation in compression mode matrix is pushed on the particle [31,32].

GMBs of three varying densities (wall thickness variations), SID-200Z, SID-270Z and SID-350Z are blended in 20, 40 and 60 vol % to form compression molded syntactic foam sheets. Neat HDPE samples

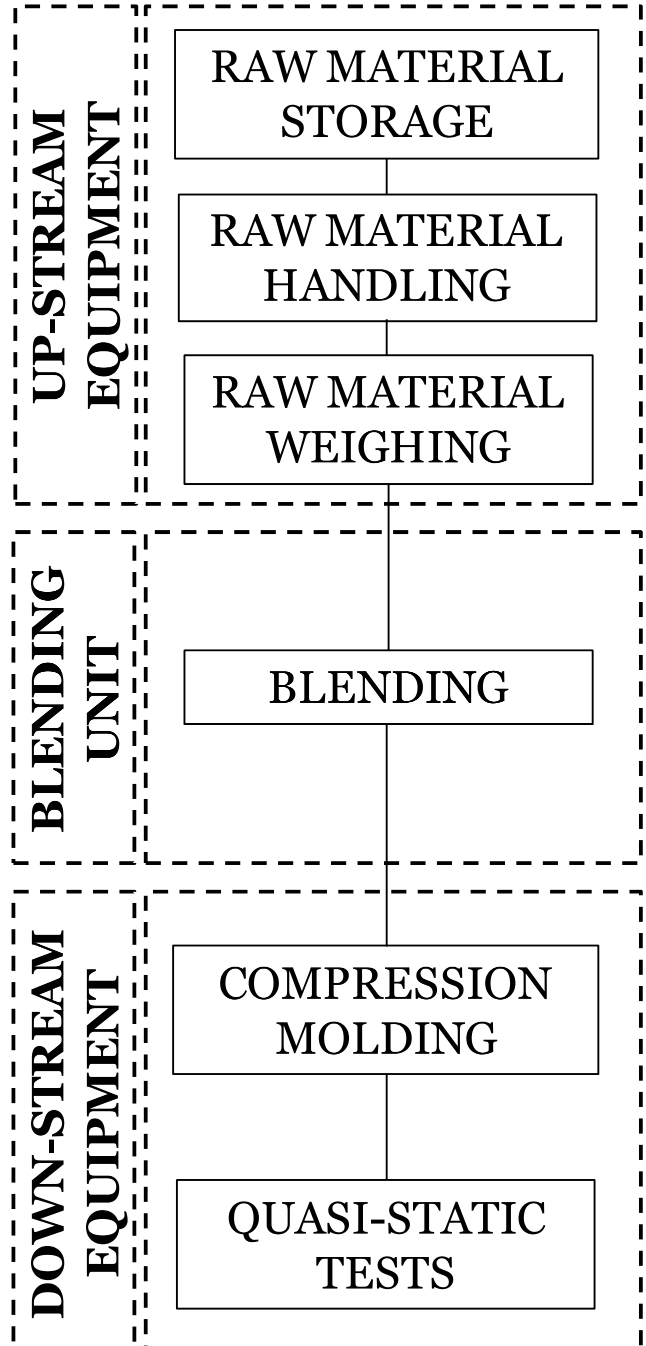

Fig. 1. Material flow and test plan.

are also prepared for comparative analysis. Manufacturing process is optimized for blending and compression molding to minimize microballoons breakage during processing [6]. Quasi static compressive properties are measured at 0.001, 0.01and 0.1s^{-1} strain rates. Stress-strain behavior, failure mechanism and energy absorption capabilities

Table 2
Physical properties of the microballoons used in the study.

Microballoon type	Collapse Pressure (psi)	Theoritical thermal conductivity (K/mK)	Average microballoon size (μm)	True particle density (kg/m^3)	Wall thickness (μm)	Radius rate (η)
SID200	1000	0.08	53	200	0.716	0.973
SID270	5000	0.10	50	270	0.925	0.963
SID350	6500	0.12	45	350	1.080	0.952

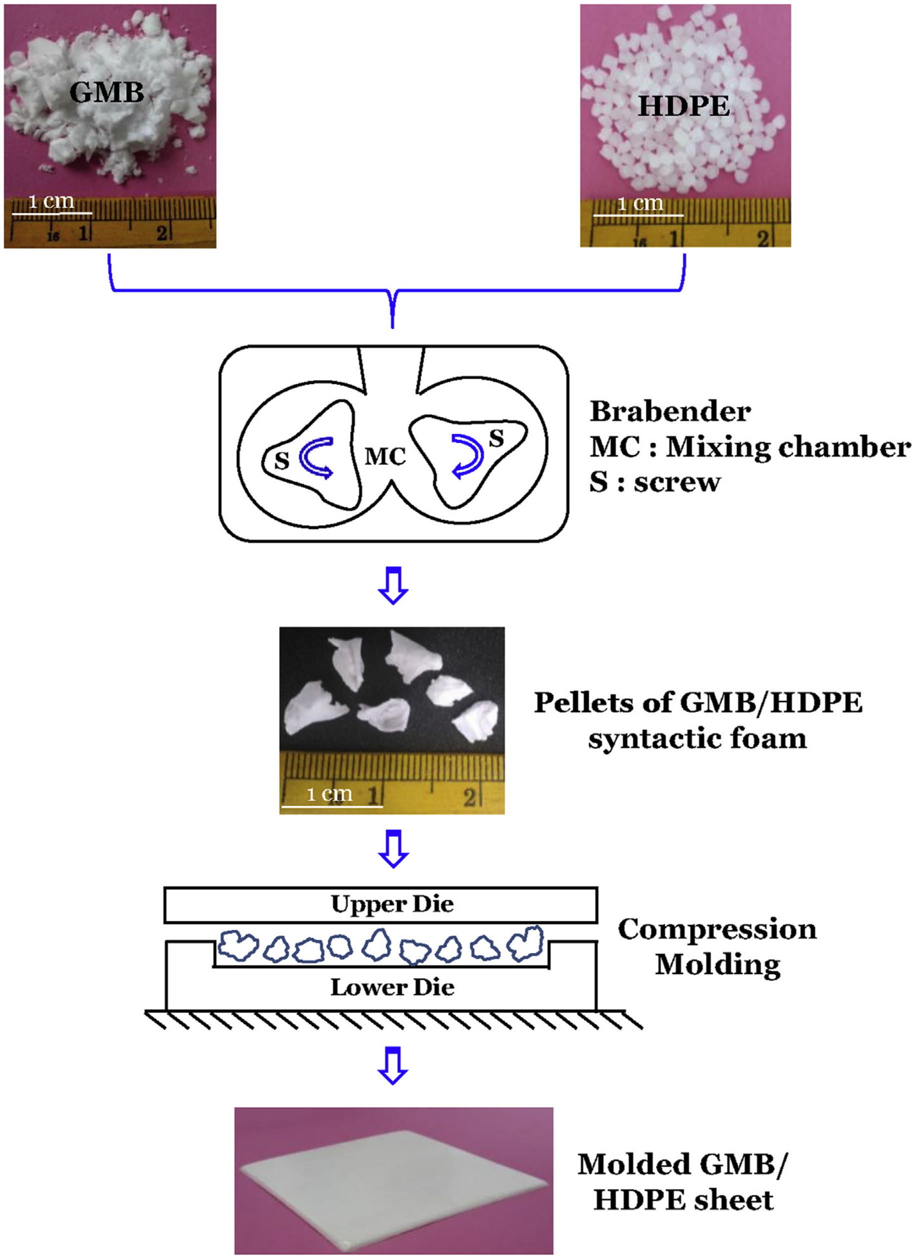

Fig. 2. Block diagram showing methodology adopted.

of these lightweight foams are presented. Fractured surface is micrographed to analyze structure-property correlations. Modulus results are validated with existing theoretical models to understand the elastic properties of glass microballoons.

2. Experimental methods

2.1. Materials and sample preparation

HDPE granules of grade 180M50 (melt flow index of 20g/10min) are procured from Indian Oil Corporaten Ltd., Mumbai, India and is used as matrix. The basic properties of HDPE are presented in Table 1. Glass microballoons with SID-200Z, SID-270Z and SID-350Z (Trelleborg, USA) having true particle densities of 200, 270 and 350 kg/m^3 respectively, are used as fillers in as received condition. Table 2 presents physical properties of GMBs used in the present work. These particles differ in densities (Table 2). Wall thickness of the GMBs is calculated using [33],

$$w = r_o (1 - \eta) \tag{1}$$

Where, r_o is the outer radius of the microballoon and η is the radius rate. Radius rate is estimated by Ref. [34],

$$\eta = \sqrt[3]{1 - \frac{\rho_{TPD}}{\rho_c}} \tag{2}$$

Where, ρ_{TPD} is the true particle density and ρ_c is the density of the glass (2540 kg/m^3 [34]). Material flow and test plan is presented in Fig. 1. Fig. 2 shows block diagram of the methodology adopted for preparing

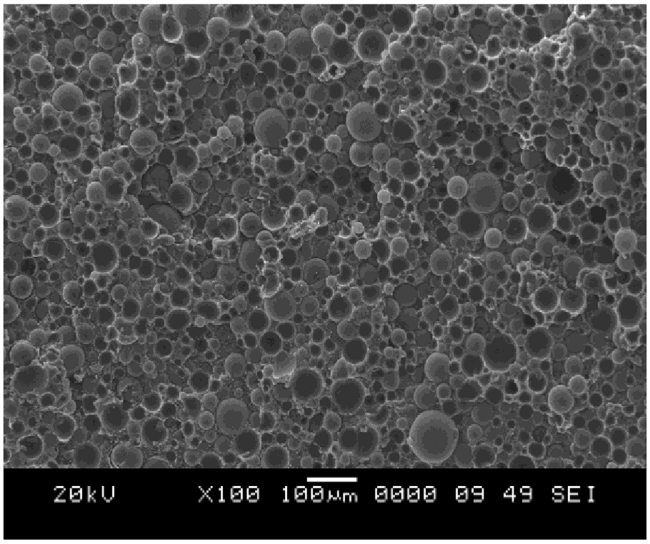

Fig. 3. Freeze-fractured micrograph of a representative GMB/HDPE sample (H200-60) showing uniform distribution of microballoons.

Table 3
Density, microballoon failure and weight saving potential of HDPE and their foams.

Material	ϕ_{gmb}(%)[a]	ρ_{exp}(kg/m^3)	ρ_{th}(kg/m^3)	GMB breakage (vol. %)	Weight saving potential (%)
H	–	950 ± 0.5	950	–	–
H200-20	20	847 ± 8	800	5.55	10.84
H200-40	40	712 ± 14	650	8.71	25.05
H200-60	60	608 ± 2	500	17.76	36
H270-20	20	845 ± 3	814	3.67	11.05
H270-40	40	727 ± 1	678	6.74	23.47
H270-60	60	642 ± 3	542	15.58	32.42
H350-20	20	853 ± 3	830	2.70	10.21
H350-40	40	741 ± 4	710	4.18	22
H350-60	60	672 ± 5	590	12.20	29.26

[a] Volume fraction of glass microballoons.

GMB/HDPE syntactic foams. Initially, GMBs and HDPE granules in as received condition are blended in Brabender. Desired proportion of GMB and HDPE are measured and loaded into the hopper of brabender machine (Plasticoder, Western company Keltron CMEI, MODEL-16CME SPL). Blending temperature (160 °C) and lobe screw rotations (10 rpm) are optimized [6] to minimize microballoons breakage. GMB/HDPE pellets from brabender are transferred to compression molding machine (SP30, Santec automation Pvt. Ltd., Delhi, India). Compression molding parameters are set at 160 °C and 50 bar pressure with total cycle time of 1.75 h [6]. In total ten (one neat HDPE and nine foam) sheets of dimension 165 × 165 × 3.2 mm are fabricated. These compression molded sheets are trimmed to 10 × 10 × 3 mm [21,35,36] dimensions and are subjected to quasi-static tests. Samples are coded according to convention HYYY-ZZ, where 'H' denotes the HDPE matrix; 'YYY' and 'ZZ' are the density and volume fraction of microballoons respectively. Microballoons breakage during processing is computed using experimental (ρ_{exp}) and theoretical (ρ_{th}) densities. Theoretical densities for all foam samples are computed using rule of mixtures while ASTM D792-13 standard is adopted to measure the experimental density of all fabricated specimens. The densities of five specimens are measured and the average values and standard deviations are reported.

2.2. Quasi-Static Compression

Z020 Zwick Roell (USA) Computer controlled universal test system with a 20-kN load cell is used for Quasi-Static Compression test at 0.001, 0.01and 0.1s^{-1} strain rates. The end of test criteria is set at 20-kN load. Flat wise load is applied on all the samples under investigation. The data is analyzed using in-house developed MATLAB code to estimate yield strength and modulus for all the samples. Average of five samples for each configuration is reported for analysis.

2.3. Imaging

JSM 6380LA, JEOL, Japan is used for micrographic analysis. The samples are sputter coated with gold using a JFC-1600 auto fine coater before imaging.

3. Results

3.1. Syntactic foam microstructure

Micrograph of representative foam samples is presented in Fig. 3. H200-60 is chosen for micrography as SID200 particles with highest filler loading (60 vol %) are prone to fail much earlier than other microballoons types (SID270 and SID350) under shear in brabender and compressive forces in compression molding. Uniform dispersion of GMB in HDPE matrix as seen from Fig. 3 affirms processing feasibility of GMB/HDPE foams as adopted in the present work. Absence of matrix porosity is clearly evident. Further, large numbers of intact microballoons are also seen. Thermoplastics are processed using high shear mixing. Though, processing parameters are optimized for quality syntactic foams, particle breakage is inevitable. As expected highest microballoons failure (17.76%) is observed in H200-60 samples (Table 3). Thinner wall thickness and higher particle-particle interactions at highest filler loadings make microballoons to fracture in H200 syntactic foams. Density of foams increases due to GMB failure. Further, increasing filler content increases GMB failure owing to higher filler interactions. Filler breakage adversely affects the mechanical properties of the syntactic foam. However even with the failed particles, fabricating syntactic foam components that are non-load-bearing can provide a substantial saving of expensive HDPE resin. Secondly, density of all foams is far lower than the neat HDPE matrix signifying weight saving potentials of these developed foams. As seen from Table 3, significant weight reduction (10–36%) is possible by using GMBs in HDPE matrix. Lower densities of foams as compared to neat HDPE matrix makes it worth investigating for quasi-static compressive response.

3.2. Experimental results

Fig. 4–6 presents the quasi-static compressive stress strain plots for neat HDPE and their foams at different strain rates. The stress-strain profile of neat HDPE processed through compression molding as presented in this study is similar to the trend observed in injection molded specimens [21]. HDPE syntactic foams exhibits different behavior as compared to thermoset foams. In vinyl ester and epoxy syntactic foams, matrix being brittle, stress drops significantly at the end of the initial linear elastic region, followed by a stress plateau [15,17]. Such stress drop is due to successive failure of brittle particles in the matrixowing to stress concentration in the localized region around broken particles [37,38]. At room temperature above Tg, HDPE is significantly more compliant and such effects are mitigated. Strain rate sensitivity is clearly evident from Fig. 4–6 for all the foams showing rise in modulus and strength with higher strain rates. Such behavior is very useful in designing materials for impact mitigation applications. Three distinct

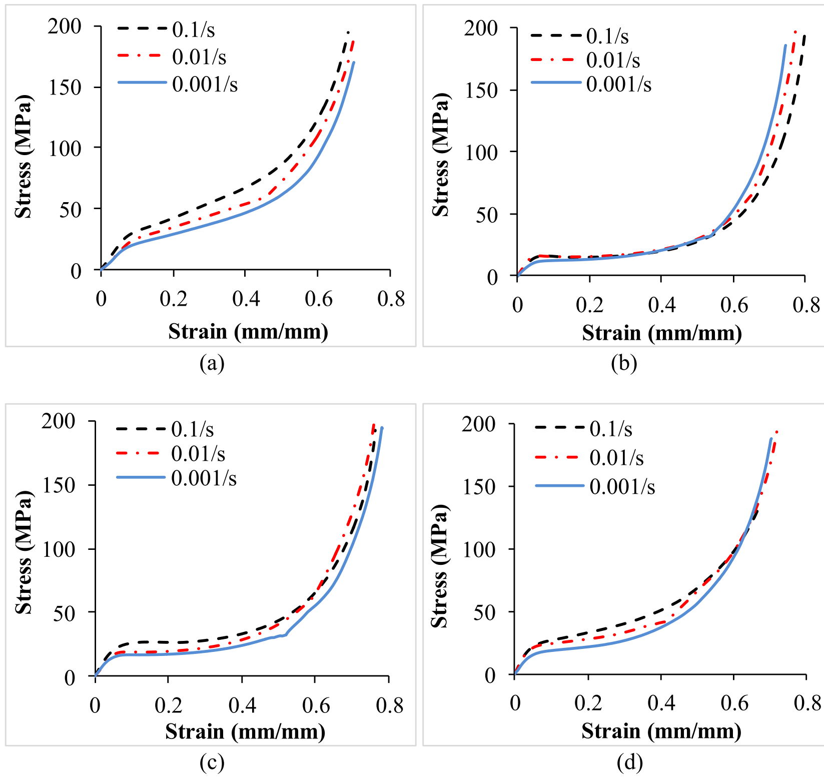

Fig. 4. Stress–strain response of (a) neat HDPE (b) H200-20 (c) H200-40 and (d) H200-60 at different strain rates.

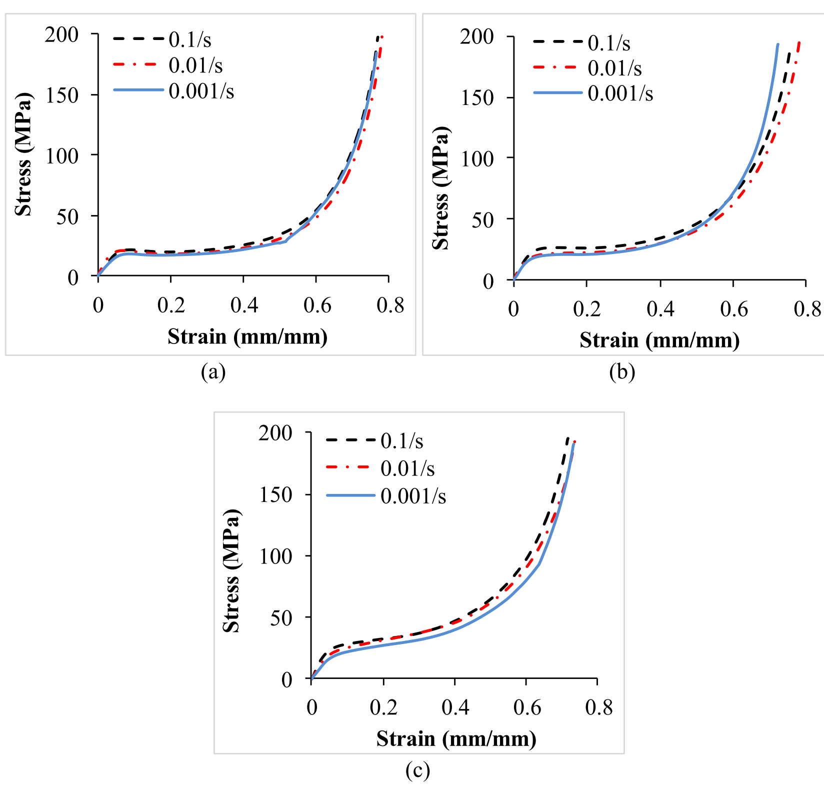

Fig. 5. Stress–strain response of (a) H270-20 (b) H270-40 and (c) H270-60 at different strain rates.

regions can be observed from representative stress-strain plots as presented in Fig. 7. These regions are (1) constant slope initial elastic region (2) a post-yield plastic deformation region with stress plateau and (3) higher and increasing slope plastic deformation region. In GMB/HDPE foams the increasing slope plastic deformation zone is named as densification region and is observed after 0.5 mm/mm strain value. In

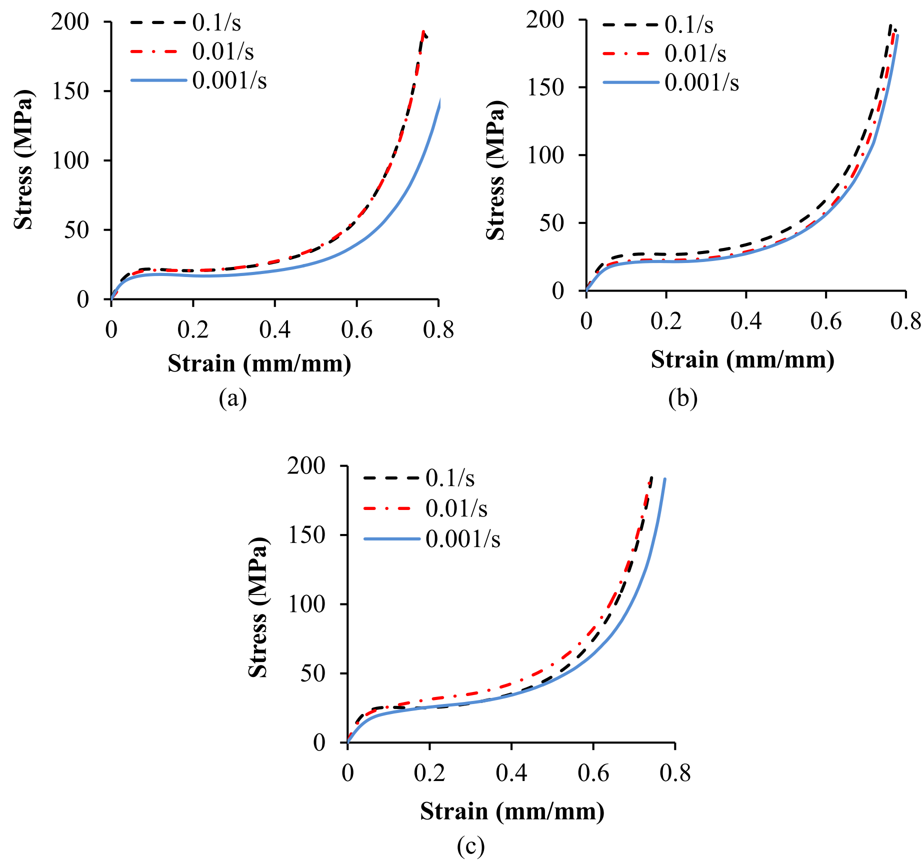

Fig. 6. Stress–strain response of (a) H350-20 (b) H350-40 and (c) H350-60 at different strain rates.

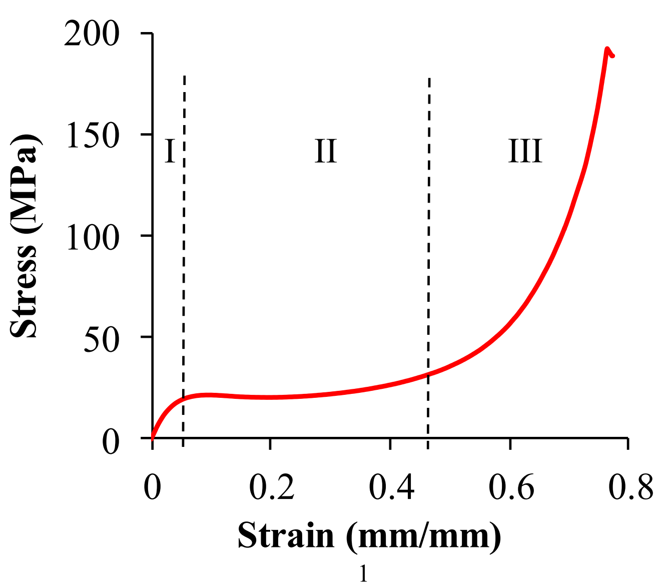

Fig. 7. Schematic stress–strain response at $0.1s^{-1}$in H350-60 showing three distinct regions (I - linear elastic, II - plateau, III - densification region) of deformation behaviour.

this region some of the stress strain responses (Fig. 4b, d, Figs. 5b and 6c) scatter in the strength values with respect to the strain rate. This attributes to the change in geometry of the crushed microballoon and the fluctuation encountered due to the presence of more void spaces within the microballoon. Lowest filler content foams exhibits clearly distinguishable stress plateau irrespective of particle wall thickness which is a characteristic of foams and porous materials (Figs. 4b, 5a and 6a). GMB reinforcement of 20 vol % in HDPE might be effective in constraining the matrix deformation. These foams can be effectively used for energy absorbing applications. Neat HDPE and other syntactic foams continue to harden at all strains.

Table 4 presents measured mechanical properties of syntactic foams. Mean elastic modulus and compressive yield strength are observed to increase with increasing strain rate for all the syntactic foams though for few standard deviation values are overlapping as seen from Fig. 8. H350-60 shows highest modulus and yield strength for all compressive strain rates among the foams investigated. GMB wall thickness has a higher influence as compared to filler volume fraction. Thick walled GMB particles have more stress resistance and higher strain energy absorption resulting in higher modulus. Thicker walled particles at higher strain rates with increasing filler content increases modulus in the range of 27–68% in comparison to neat HDPE (Table 4). Neat HDPE registered maximum yield strength of 34.92 MPa at highest strain rate as compared to all the syntactic foams developed in the present study. Nevertheless, specific properties need to be looked into from weight saving perspective. Yield strength is seen to be increasing with particle wall thickness and strain rate as evident from Fig. 9. Increasing filler content decreases yield strength to the tune of 17–39, 24–36 and 12–36% respectively at 0.001, 0.01 and $0.1s^{-1}$ strain rate for H200, H270 and H350 as compared to neat matrix. Higher energy absorption capabilities are noted in thicker walled foams. Table 5

Table 4
Mechanical properties for HDPE and their foams.

Material	Strain rate (s-1)	Modulus (MPa)	Yield strength (MPa)	Yield strain (%)	Energy absorbed to 40% strain (MJ/m^3)	Densification Stress (MPa)	Densification Strain (%)
H	0.001	226.31 ± 11.31	29.47 ± 1.47	2.25 ± 0.11	14.71 ± 0.74	–	–
	0.01	289.60 ± 14.48	32.58 ± 1.63	3.72 ± 0.19	16.63 ± 0.83	–	–
	0.1	350.52 ± 20.47	34.92 ± 1.75	4.19 ± 0.21	17.99 ± 0.90	–	–
H200-20	0.001	330.70 ± 16.53	21.94 ± 1.09	1.99 ± 0.10	10.81 ± 0.54	42.79 ± 2.14	49.37 ± 2.46
	0.01	373.30 ± 18.66	26.23 ± 1.31	2.45 ± 0.12	13.29 ± 0.67	48.19 ± 2.41	41.45 ± 2.07
	0.1	410.43 ± 20.52	26.99 ± 1.35	2.12 ± 0.11	10.96 ± 0.55	54.64 ± 2.73	58.07 ± 2.91
H200-40	0.001	368.99 ± 18.45	19.89 ± 0.99	1.70 ± 0.09	8.79 ± 0.44	41.78 ± 2.08	55.32 ± 2.76
	0.01	393.71 ± 19.68	21.43 ± 1.07	1.72 ± 0.09	9.81 ± 0.49	61.49 ± 3.07	59.26 ± 2.96
	0.1	469.50 ± 23.47	24.73 ± 1.24	2.62 ± 0.13	11.06 ± 0.55	63.70 ± 3.18	59.45 ± 2.97
H200-60	0.001	395.23 ± 19.76	18.05 ± 0.92	1.56 ± 0.08	7.56 ± 0.38	35.93 ± 1.79	54.68 ± 2.73
	0.01	423.21 ± 21.15	21.00 ± 1.05	2.23 ± 0.11	10.08 ± 0.50	55.85 ± 2.79	59.27 ± 2.96
	0.1	511.30 ± 25.56	22.35 ± 1.12	2.50 ± 0.12	8.47 ± 0.42	55.30 ± 2.76	63.90 ± 3.19
H270-20	0.001	353.10 ± 17.65	23.74 ± 1.19	1.89 ± 0.09	11.55 ± 0.58	61.06 ± 3.05	54.03 ± 2.70
	0.01	434.38 ± 21.71	27.77 ± 1.39	1.95 ± 0.09	13.71 ± 0.69	80.03 ± 4.01	56.87 ± 2.84
	0.1	453.20 ± 22.66	29.71 ± 1.48	2.58 ± 0.13	15.11 ± 0.76	82.46 ± 4.12	56.44 ± 2.82
H270-40	0.001	398.40 ± 19.92	21.62 ± 1.09	1.52 ± 0.08	10.33 ± 0.52	41.60 ± 2.08	49.30 ± 2.46
	0.01	423.12 ± 21.15	25.88 ± 1.29	3.13 ± 0.16	10.31 ± 0.52	46.40 ± 2.32	53.24 ± 2.66
	0.1	528.30 ± 26.41	27.90 ± 1.39	2.31 ± 0.12	12.32 ± 0.62	68.35 ± 3.41	59.50 ± 2.97
H270-60	0.001	403.00 ± 20.15	22.29 ± 1.11	2.11 ± 0.11	8.83 ± 0.44	32.65 ± 1.63	56.44 ± 2.82
	0.01	483.30 ± 24.16	24.10 ± 1.21	1.61 ± 0.08	9.59 ± 0.48	41.38 ± 2.06	51.34 ± 2.56
	0.1	590.23 ± 29.51	25.30 ± 1.27	2.66 ± 0.13	10.17 ± 0.51	62.34 ± 3.11	62.26 ± 3.11
H350-20	0.001	368.60 ± 18.43	24.46 ± 1.22	1.91 ± 0.09	13.28 ± 0.66	59.71 ± 2.98	58.32 ± 2.91
	0.01	435.28 ± 21.76	27.36 ± 1.36	2.29 ± 0.11	14.20 ± 0.71	75.58 ± 3.77	57.99 ± 2.90
	0.1	500.15 ± 26.61	30.81 ± 1.54	3.04 ± 0.15	14.33 ± 0.72	80.04 ± 4.01	61.42 ± 3.07
H350-40	0.001	410.06 ± 19.01	23.37 ± 1.17	2.16 ± 0.11	10.18 ± 0.51	48.83 ± 2.44	56.87 ± 2.84
	0.01	505.39 ± 25.27	24.35 ± 1.21	2.02 ± 0.10	11.10 ± 0.56	59.74 ± 2.98	60.48 ± 3.02
	0.1	562.03 ± 27.10	28.22 ± 1.41	2.46 ± 0.12	12.44 ± 0.62	66.08 ± 3.31	59.64 ± 2.98
H350-60	0.001	480.90 ± 20.09	22.99 ± 1.15	2.07 ± 0.10	9.49 ± 0.48	31.90 ± 1.59	55.19 ± 2.76
	0.01	573.25 ± 28.66	24.75 ± 1.24	1.45 ± 0.07	9.54 ± 0.48	27.35 ± 1.36	47.69 ± 2.38
	0.1	689.01 ± 34.45	26.64 ± 1.33	2.71 ± 0.13	10.61 ± 0.53	52.89 ± 2.64	58.58 ± 2.93

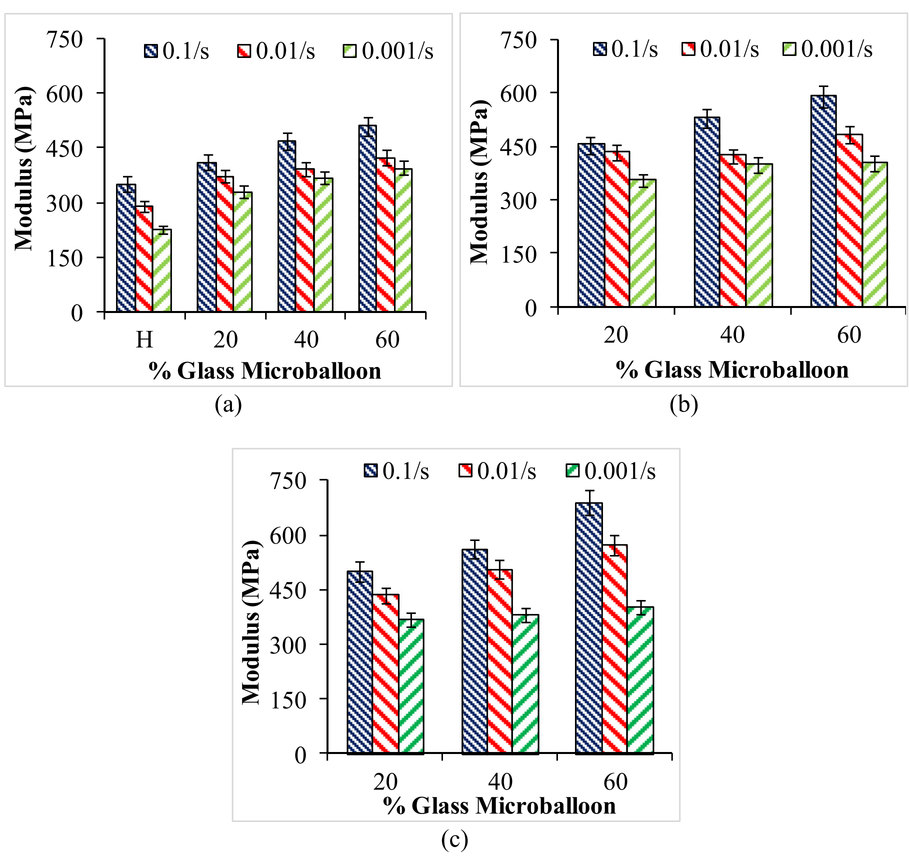

Fig. 8. Experimentally measured modulus for (a) neat HDPE and H200 (b) H270 and (c) H350 at different compressive strain rates.

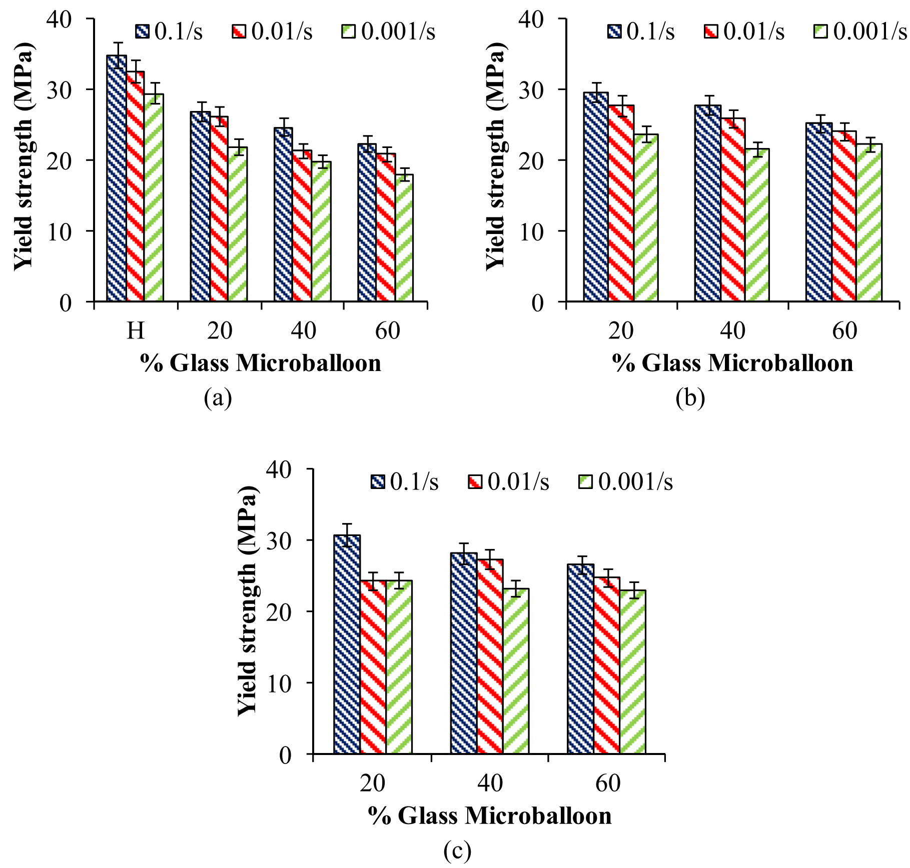

Fig. 9. Experimentally measured yield strength for (a) neat HDPE andH200 (b) H270 and (c) H350 at different compressive strain rates.

Table 5
Specific compressive properties for HDPE and their foams.

Material	Strain rate (s^{-1})	Specific compressive Modulus (MPa/kg/m^3)	Specific compressive Yield strength (MPa/kg/m^3) × 10^{-3}
H	0.001	0.238	31.02
	0.01	0.305	34.29
	0.1	0.431	36.75
H200-20	0.001	0.390	25.90
	0.01	0.441	30.97
	0.1	0.485	31.87
H200-40	0.001	0.518	27.94
	0.01	0.553	30.10
	0.1	0.659	34.73
H200-60	0.001	0.650	29.68
	0.01	0.696	34.54
	0.1	0.891	36.76
H270-20	0.001	0.42	28.09
	0.01	0.50	29.74
	0.1	0.54	34.72
H270-40	0.001	0.55	32.86
	0.01	0.60	35.60
	0.1	0.73	37.54
H270-60	0.001	0.63	35.16
	0.01	0.75	38.38
	0.1	0.92	39.41
H350-20	0.001	0.43	28.09
	0.01	0.51	32.86
	0.1	0.62	35.16
H350-40	0.001	0.51	28.55
	0.01	0.68	36.92
	0.1	0.73	36.83
H350-60	0.001	0.60	36.12
	0.01	0.85	38.08
	0.1	1.03	39.64

presents specific compressive modulus and yield strengths for various material compositions. All syntactic foams registered superior performance compared to neat HDPE for specific modulus (0.39–1.03 MPa/kg/m^3) at all strain rates (Fig. 10). While higher filler loading resulted in higher specific strength values compared to HDPE matrix as seen from Fig. 11. Reducing filler breakage further might lead to higher specific yield strengths even at lower filler contents. Highest specific modulus (1.03 MPa/kg/m^3) and yield strength (0.03964 MPa/kg/m^3) is observed for H350-60. These finding implies that, H350-60 foam is useful in reducing thermoplastic resin usage a given applications with overall weight saving of 29.26% (Table 3).

Table 4 presents measured densification strain and corresponding stresses for all the syntactic foams [39]. The densification strain and their corresponding stress values increases as strain rate increases for all syntactic foams. Effect of particle wall thickness and volume fraction did not show any specific trend pertaining to densification values. Fig. 12 presents SEM images of the compressed samples at lower and higher strain rates for all syntactic foams. Intact microballoons are observed post densification in all the samples (Fig. 12). High strength bearing thicker walled particles (Fig. 12g–l) are survived more in number compared to thinners walled (Fig. 12a– f) ones. Fig. 12a– f exhibits extensive matrix deformation and debris as compared to Fig. 12g–l. Change in strain rate magnitude did not show any distinct change in failure features as observed from these micrographs. Nevertheless, these failure features might help in analyzing failure patterns post high strain rate test.

3.3. Theoretical modeling

Elastic properties of syntactic foams can be estimated using several available theoretical models [40]. Experimental results are found to be in close agreement with the values predicted by these theoretical

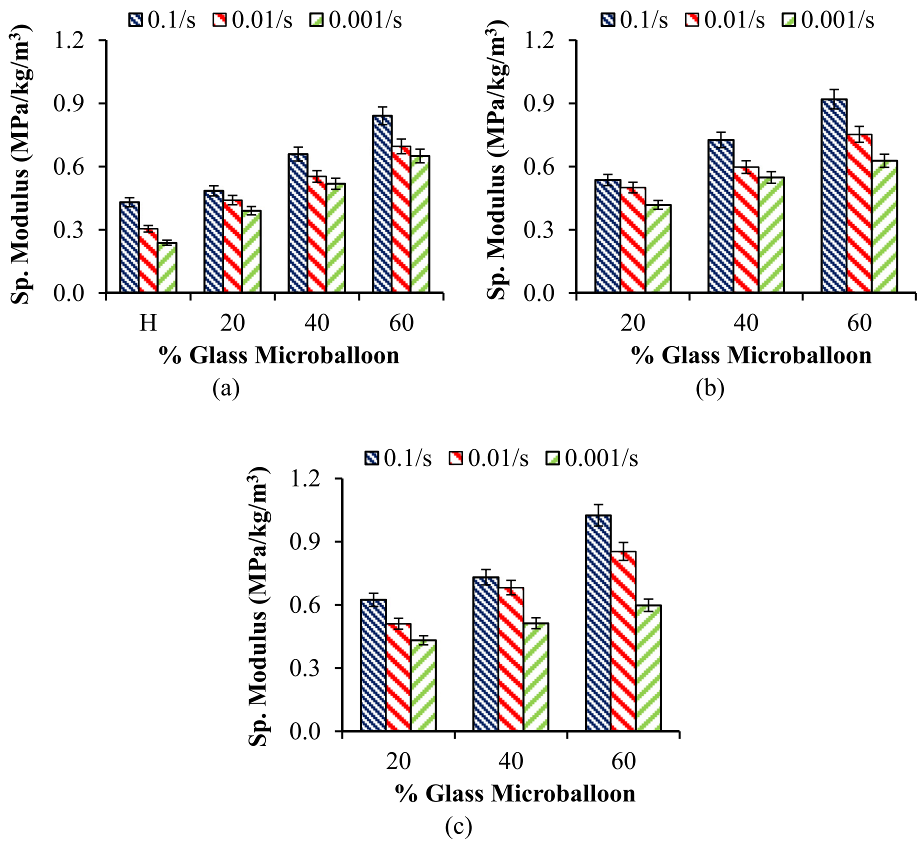

Fig. 10. Experimentally measured specific modulus for (a) neat HDPE and H200 (b) H270 and (c) H350 at different compressive strain rates.

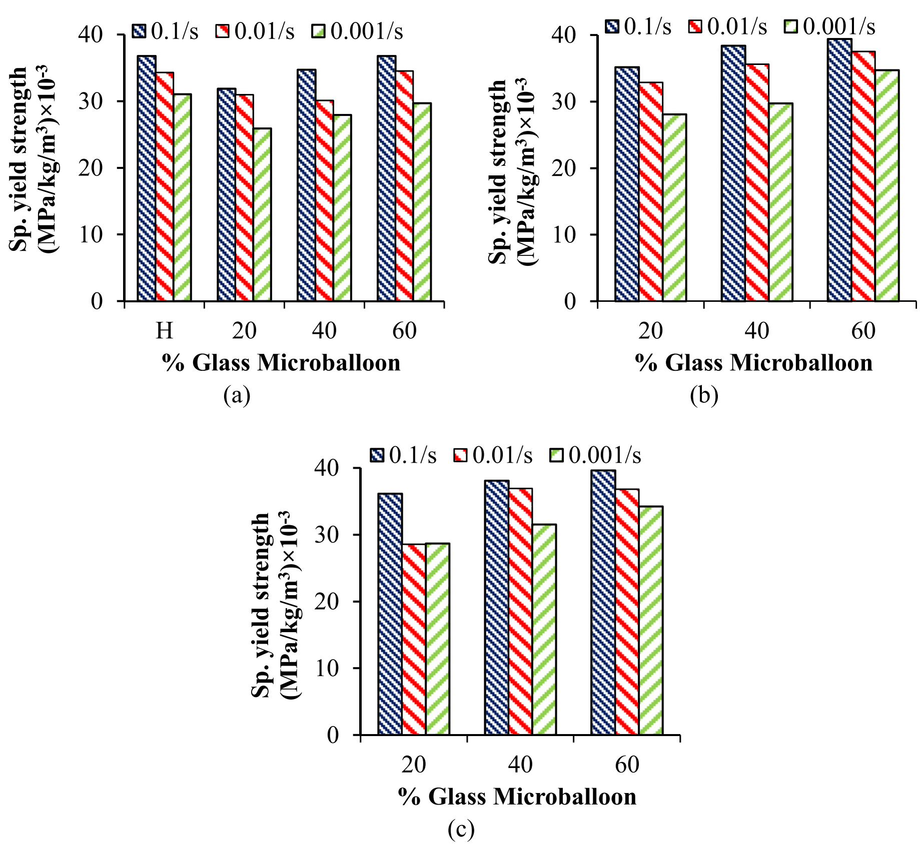

Fig. 11. Experimentally measured specific yield strength for (a) neat HDPE and H200 (b) H270 and (c) H350 at different compressive strain rates.

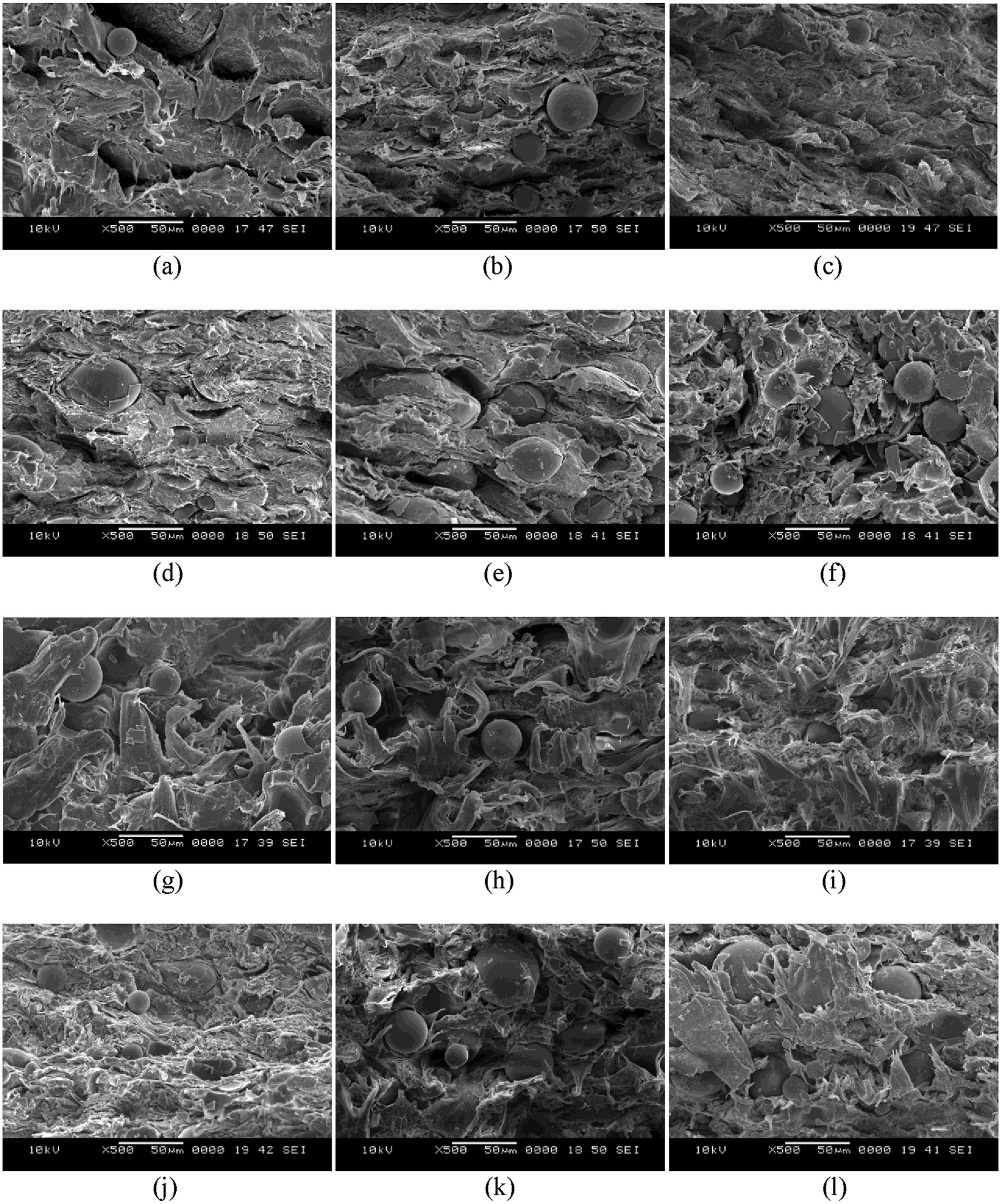

Fig. 12. SEM image of compressed Syntactic foam samples of (a) H200-20 specimen at 0.001s^{-1}, (b) H200-20 specimen at 0.1s^{-1}(c) H200-40 specimen at 0.001s^{-1}(d) H200-40 specimen at 0.1s^{-1}(e) H200-60 specimen at 0.001s^{-1}(f) H200-60 specimen at 0.1s^{-1}(g) H350-20 specimen at 0.001s^{-1}(h) H350-20 specimen at 0.1s^{-1} (i) H350-40 specimen at 0.001s^{-1} (j) H350-40 specimen at 0.1s^{-1} (k) H350-60 specimen at 0.001s^{-1} and (l) H350-60 specimen at 0.1s^{-1}. Survived GMB particles after densification are clearly evident from these micrographs.

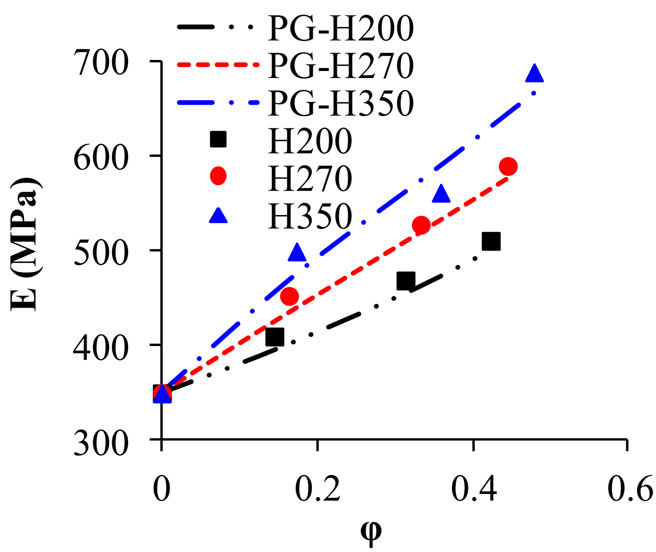

Fig. 13. Comparison of experimental and theoretical values for compressive modulus.

models developed for thermosetting syntactic foams [31]. Analysis of cenosphere filled thermoplastic foams is carried out using one of these models based on a differential scheme [31,41] of Porfiri-Gupta model. The differential scheme is as follows,

$$\frac{dE}{E} = f_E(E_i, v_i, E_m, v_m, \eta)\frac{d\Phi_f}{1-\Phi_f/\Phi_m} \tag{3}$$

where E_i and v_i are the young's modulus and Poisson's rate of the microballoon material, E_m and v_m are the modulus and Poisson's rate of the matrix material. Φ_f represents microballoon volume fraction and Φ_m denotes the maximum packing factor of particles (assumed to be 0.637 [42]). For modeling, modulus of the matrix material is taken from the experimental result of compression test carried out for a strain rate of $0.1 s^{-1}$ and Poisson's rate is assumed to be 0.425 [43]. Modulus of the microballoon is assumed to be 60 GPa with a Poisson's rate 0.21 [32]. The parameter η is the radius rate of the hollow particles (rate of the inner radius to outer radius) and is listed in Table 2. Using differential scheme compression modulus is estimated for all types of GMB/HDPE syntactic foams by varying Φ_f and η. Varying Φ_f and η, compression modulus is calculated for all types of GMB/HDPE syntactic foams at constant strain rate. Model is analyzed for strain rates 0.001, 0.01 and 0.1/s. It is observed that compressive modulus is increased with an increase of filler content and wall thickness. The comparison between Porfiri-Gupta model and experimental results for 0.1/s strain rate is presented in Fig. 13. Theoretical model takes into account particles survived (Table 3) for estimation compressive modulus. Experimental results are found to be in good agreement with theoretical ones (less than 5%) though slight deviations are noted as seen from Fig. 13. Such deviations might be due to wall thickness variation in the microballoon shells. These models comes handy to predict properties beforehand partially saving experimental efforts.

3.4. Property map

Quasi-static compressive strength and modulus values are plotted with respect to density for thermoplastic foams containing different reinforcements tested at strain rates of 0.001 and 0.01 s^{-1} are presented in Fig. 14a [21,44–48] and Fig. 14b, [21]. The results extracted from the published literature are presented and compared with the present study. Present study shows that, GMB/HDPE foam is having lower density possessing high compressive strength compared to the published literature. H270-20 at $0.01 s^{-1}$ strain rate exhibits superior compressive strength. Density of GMB/HDPE foams is observed to be 1.75 times lower as compared with cenosphere/HDPE foams for 0.001 and $0.01 s^{-1}$ strain rate. H350-60 at 0.01 s^{-1} strain rate exhibits higher modulus compared to other published work [21,44–48]. Choice of appropriate filler and the matrix tailored the compression properties of the foams over a wide range as seen from Fig. 14. Such property maps come handy and useful for selection of particular foam for a given application.

4. Conclusions

Present work deals with developing lightweight syntactic foams using industrial scale compression molding route and analysing effect of wall thickness variation and filler loading on strain rate. Brabender blending and compression molding is used to synthesize HDPE syntactic foams containing 20, 40 and 60 vol % glass microballoons of different densities. Quasi-static compression tests are conducted on these GMB/HDPE syntactic foams. Porfiri-Gupta model is used to estimate and compare the theoretical values with the experimental data of syntactic foams. The results of the study can be summarized as:

- Adopted methodology for processing of GMB/HDPE syntactic foams using compression molding is successfully potential up to 36% is achieved in the present work.
- Compressive modulus and yield strength are strain rate sensitive properties showing rise with increasing strain rates.
- Neat HDPE and other syntactic foams with higher filler loading continue to harden at all strains except H200 foams which exhibits clearly distinguishable stress plateau irrespective of particle wall thickness. These foams can be effectively used for energy absorbing applications.
- All syntactic foams registered superior performance compared to neat HDPE for specific modulus at all strain rates. H350-60 shows highest modulus and yield strength for all compressive strain rates among the foams investigated.
- GMB wall thickness has a higher influence as compared to volume fraction for the properties investigated in the present work.
- Theoretical approach by Porfiri-Gupta model is found to be in good agreement (less than 5%) with experimental results.
- Compressive strength of GMB/HDPE foams exhibited better results (except H200-60) compare to other polymeric foams in the literature. H350-60 exhibited better modulus as compared to other available thermoplastic foams.

Compression molding results in better quality syntactic foams i.e. higher strength (except H200-60) and modulus (H350-60) as compared to Injection molding processing route. Further, wall thickness has a strong influence on quasi-static behavior of GMB/HDPE foams. In addition to filler volume fraction, wall thickness variation results in wider range of compressive properties which can cater to different sectors based on the application. Present work provides guideline to polymer industries in developing GMB based polymeric foams without changing existing machine parameters and their setups.

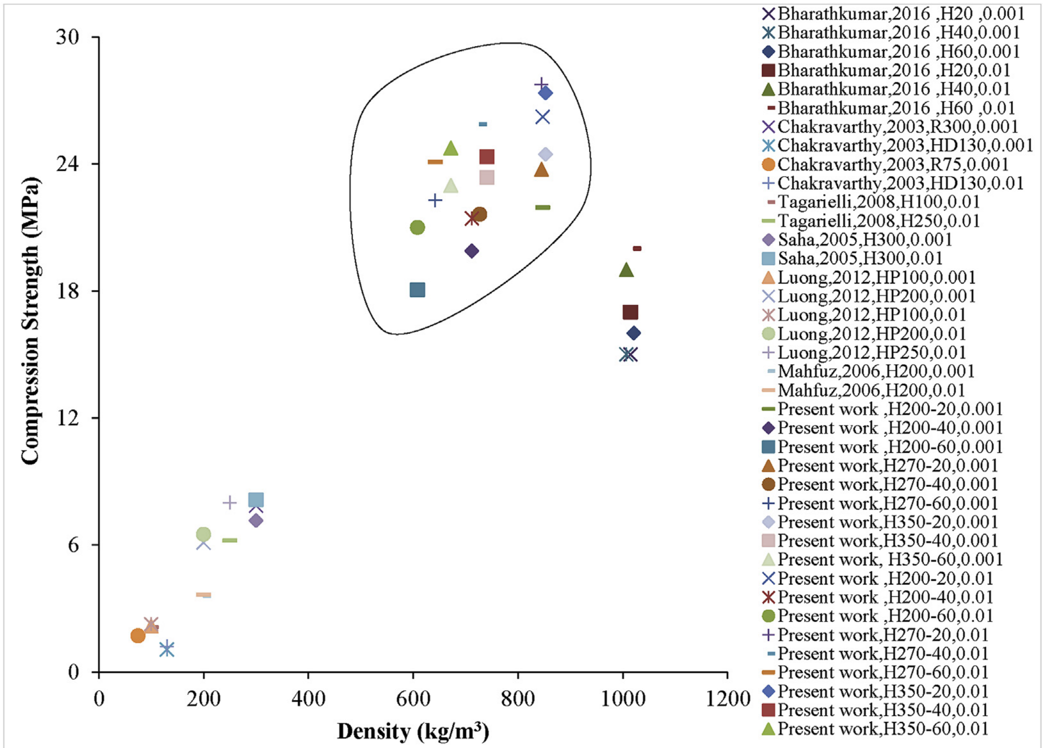

(a)

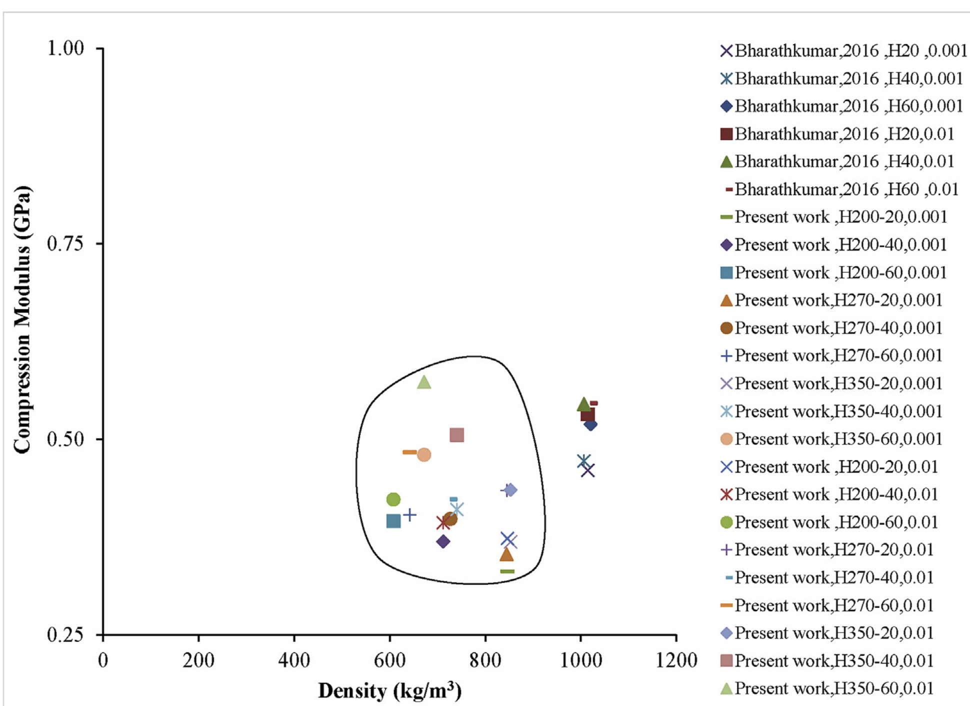

(b)

Fig. 14. Compressive strength and modulus of thermoplastic composites plotted against density from available studies [21], [44–48].

Acknowledgements

Department of Science and Technology, Government of India, Technology Systems Development Program grant DST/TSG/AMT/2015/394/G is acknowledged by Mrityunjay Doddamani. The views expressed in this article are those of authors, not of funding agencies. The authors thank the ME Department at NIT-K for providing facilities and support.

References

[1] Yalcin B, Amos SE. 3-Hollow glass microspheres in thermoplastics. Hollow glass microspheres for plastics, elastomers, and adhesives compounds. Oxford: William Andrew Publishing; 2015. p. 35–105.
[2] DeArmitt C. 23-Functional fillers for plastics A2-Kutz, Myer. Applied plastics engineering handbook. second ed.William Andrew Publishing; 2017. p. 517–32.
[3] Rothon R, Hornsby P. Chapter 9-fire retardant fillers for polymers. Polymer Green flame retardants. Amsterdam: Elsevier; 2014. p. 289–321.
[4] Höfer R. 10.21-Processing and performance Additives for plastics A2-Matyjaszewski, Krzysztof. In: Möller M, editor. Polymer science: a comprehensive reference. Amsterdam: Elsevier; 2012. p. 369–81.
[5] Shutov F. Syntactic polymer foams. Chromatography/foams/copolymers. 1986. p. 63–123.
[6] Jayavardhan ML, Bharath Kumar BR, Doddamani M, Singh AK, Zeltmann SE, Gupta N. Development of glass microballoon/HDPE syntactic foams by compression molding. Compos B Eng 2017;130(Supplement C):119–31.
[7] Gupta N, Singh Brar B, Woldesenbet E. Effect of filler addition on the compressive and impact properties of glass fibre reinforced epoxy. Bull Mater Sci 2001;24(2):219–23.
[8] Grosjean F, Bouchonneau N, Choqueuse D, Sauvant-Moynot V. Comprehensive analyses of syntactic foam behaviour in deepwater environment. J Mater Sci 2009;44(6):1462–8.
[9] Doddamani M, Kishore VC, Shunmugasamy, Gupta N, Vijayakumar HB. Compressive and flexural properties of functionally graded fly ash cenosphere–epoxy resin syntactic foams. Polym Compos 2015;36(4):685–93.
[10] Rohatgi PK, Weiss D, Gupta N. Applications of fly ash in synthesizing low-cost MMCs for automotive and other applications. JOM (J Occup Med) 2006;58(11):71–6.
[11] Kumar BRB, Doddamani M, Zeltmann SE, Gupta N, Ramakrishna S. Data characterizing tensile behavior of cenosphere/HDPE syntactic foam. Data in Brief 2016;6:933–41.
[12] Palumbo M, Donzella G, Tempesti E, Ferruti P. On the compressive elasticity of epoxy resins filled with hollow glass microspheres. J Appl Polym Sci 1996;60(1):47–53.
[13] van Belle, B., Advances in high-temperature syntactic foam technology for offshore systems. Offshore Technology conference.
[14] Tres PA. Hollow glass microspheres stronger spheres tackle injection molding. Plast Technol 2007;53(5):6.
[15] Swetha C, Kumar R. Quasi-static uni-axial compression behaviour of hollow glass microspheres/epoxy based syntactic foams. Mater Des 2011;32(8):4152–63.
[16] Zhang X, Wang P, Zhou Y, Li X, Yang E-H, Yu TX, Yang J. The effect of strain rate and filler volume fraction on the mechanical properties of hollow glass microsphere modified polymer. Compos B Eng 2016;101(Supplement C):53–63.
[17] Gupta N, Ye R, Porfiri M. Comparison of tensile and compressive characteristics of vinyl ester/glass microballoon syntactic foams. Compos B Eng 2010;41(3):236–45.
[18] Gupta N, Woldesenbet E. Hygrothermal studies on syntactic foams and compressive strength determination. Compos Struct 2003;61(4):311–20.
[19] Yang S, Taha-Tijerina J, Serrato-Diaz V, Hernandez K, Lozano K. Dynamic mechanical and thermal analysis of aligned vapor grown carbon nanofiber reinforced polyethylene. Compos B Eng 2007;38(2):228–35.
[20] *7-Polyethylene*, HDPE, in Chemical resistance of thermoplastics. 2012, William Andrew Publishing: Oxford. p. 582–1295.
[21] Bharath Kumar BR, Singh AK, Doddamani M, Luong DD, Gupta N. Quasi-static and high strain rate compressive response of injection-molded cenosphere/HDPE syntactic foam. JOM (J Occup Med) 2016;68(7):1861–71.
[22] Zeltmann SE, Prakash KA, Doddamani M, Gupta N. Prediction of modulus at various strain rates from dynamic mechanical analysis data for polymer matrix composites. Compos B Eng 2017;120(Supplement C):27–34.
[23] Bharath Kumar BR, Zeltmann SE, Doddamani M, Gupta N, Gurupadu Uzma S, Sailaja RRN. Effect of cenosphere surface treatment and blending method on the tensile properties of thermoplastic matrix syntactic foams. J Appl Polym Sci 2016(35):133. [p. n/a-n/a].
[24] Luong DD, Strbik III OM, Hammond VH, Gupta N, Cho K. Development of high performance lightweight aluminum alloy/SiC hollow sphere syntactic foams and compressive characterization at quasi-static and high strain rates. J Alloy Comp 2013;550:412–22.
[25] Luong DD, Shunmugasamy VC, Gupta N, Lehmhus D, Weise J, Baumeister J. Quasi-static and high strain rates compressive response of iron and Invar matrix syntactic foams. Mater Des 2015;66:516–31.
[26] Santa Maria JA, Schultz BF, Ferguson J, Gupta N, Rohatgi PK. Effect of hollow sphere size and size distribution on the quasi-static and high strain rate compressive properties of Al-A380–Al2O3 syntactic foams. J Mater Sci 2014;49(3):1267–78.
[27] Ahmadi H, Liaghat G, Shokrieh M, Hadavinia H, Ordys A, Aboutorabi A. Quasi-static and dynamic compressive properties of ceramic microballoon filled syntactic foam. J Compos Mater 2015;49(10):1255–66.
[28] Bharath Kumar BR, Doddamani M, Zeltmann SE, Gupta N, Gurupadu Uzma S, Sailaja RRN. Effect of surface treatment and blending method on flexural properties of injection molded cenosphere/HDPE syntactic foams. J Mater Sci 2016;51(8):3793–805.
[29] Zhang L, Ma J. Effect of coupling agent on mechanical properties of hollow carbon microsphere/phenolic resin syntactic foam. Compos Sci Technol 2010;70(8):1265–71.
[30] Yusriah L, Mariatti M. Effect of hybrid phenolic hollow microsphere and silica-filled vinyl ester composites. J Compos Mater 2013;47(2):169–82.
[31] Aureli M, Porfiri M, Gupta N. Effect of polydispersivity and porosity on the elastic properties of hollow particle filled composites. Mech Mater 2010;42(7):726–39.
[32] Tagliavia G, Porfiri M, Gupta N. Analysis of flexural properties of hollow-particle filled composites. Compos B Eng 2010;41(1):86–93.
[33] Gupta N, Ricci W. Comparison of compressive properties of layered syntactic foams having gradient in microballoon volume fraction and wall thickness. Mater Sci Eng, A 2006;427(1–2):331–42.
[34] Gupta N, Woldesenbet E, Mensah P. Compression properties of syntactic foams: effect of cenosphere radius rate and specimen aspect rate. Compos Appl Sci Manuf 2004;35(1):103–11.
[35] Li P, Petrinic N, Siviour C, Froud R, Reed J. Strain rate dependent compressive properties of glass microballoon epoxy syntactic foams. Mater Sci Eng, A 2009;515(1–2):19–25.
[36] Gupta N, Zeltmann SE, Luong DD, Doddamani M. Schmauder S, Chen C-S, Chawla KK, Chawla N, Chen W, Kagawa Y, editors. Testing of foams, in handbook of mechanics of materials. Singapore: Springer Singapore; 2018. p. 1–40.
[37] Kim JI, Ryu SH, Chang YW. Mechanical and dynamic mechanical properties of waste rubber powder/HDPE composite. J Appl Polym Sci 2000;77(12):2595–602.
[38] Wong CP, Bollampally RS. Thermal conductivity, elastic modulus, and coefficient of thermal expansion of polymer composites filled with ceramic particles for electronic packaging vol. 74. Hoboken, NJ: ETATS-UNIS: Wiley; 1999.
[39] Smith B, Szyniszewski S, Hajjar J, Schafer B, Arwade S. Characterization of steel foams for structural components. Metals 2012;2(4):399.
[40] Luong DD, Gupta N, Daoud A, Rohatgi PK. High strain rate compressive characterization of aluminum alloy/fly ash cenosphere composites. JOM (J Occup Med) 2011;63(2):53–6.
[41] Porfiri M, Gupta N. Effect of volume fraction and wall thickness on the elastic properties of hollow particle filled composites. Compos B Eng 2009;40(2):166–73.
[42] Torquato S. Random heterogeneous materials - microstructure and macroscopic properties. Interdisciplinary applied mathematics. New York: Springer; 2002.
[43] Bharath Kumar BR, Doddamani M, Zeltmann SE, Gupta N, Ramesh MR, Ramakrishna S. Processing of cenosphere/HDPE syntactic foams using an industrial scale polymer injection molding machine. Mater Des 2016;92:414–23.
[44] Chakravarty U, Mahfuz H, Saha M, Jeelani S. Strain rate effects on sandwich core materials: an experimental and analytical investigation. Acta Mater 2003;51(5):1469–79.
[45] Tagarielli V, Deshpande V, Fleck N. The high strain rate response of PVC foams and end-grain balsa wood. Compos B Eng 2008;39(1):83–91.
[46] Luong DD, Pinisetty D, Gupta N. Compressive properties of closed-cell polyvinyl chloride foams at low and high strain rates: experimental investigation and critical review of state of the art. Compos B Eng 2013;44(1):403–16.
[47] Mahfuz H, Thomas T, Rangari V, Jeelani S. On the dynamic response of sandwich composites and their core materials. Composites science and technology. 2006;66(14):2465–72.
[48] Saha M, Mahfuz H, Chakravarty U, Uddin M, Kabir ME, Jeelani S. Effect of density, microstructure, and strain rate on compression behavior of polymeric foams. Mater Sci Eng, A 2005;406(1):328–36.